Water Dispersible and Biocompatible Porphyrin-Based Nanospheres for Biophotonics Applications: A Novel Surfactant and Polyelectrolyte-Based Fabrication Strategy for Modifying Hydrophobic Porphyrins

Ning Sheng,[†,‡] Shenfei Zong,[†] Wei Cao,[§] Jianzhuang Jiang,[§] Zhuyuan Wang,[†] and Yiping Cui*,[†]

[†]Advanced Photonics Center, Southeast University, Nanjing 210096, PR China

[‡]Key Laboratory of Inorganic Chemistry in Universities of Shandong, Department of Chemistry and Chemical Engineering, Jining University, Qufu, 273155, PR China

[§]Beijing Key Laboratory for Science and Application of Functional Molecular and Crystalline Materials, Department of Chemistry, University of Science and Technology Beijing, Beijing 100083, PR China

S *Supporting Information*

ABSTRACT: The hydrophobility of most porphyrin and porphyrin derivatives has limited their applications in medicine and biology. Herein, we developed a novel and general strategy for the design of porphyrin nanospheres with good biocompatibility and water dispersibility for biological applications using hydrophobic porphyrins. In order to display the generality of the method, we used two hydrophobic porphyrin isomers as starting material which have different structures confirmed by an X-ray technique. The porphyrin nanospheres were fabricated through two main steps. First, the uniform porphyrin nanospheres stabilized by surfactant were prepared by an interfacially driven microemulsion method, and then the layer-by-layer method was used for the synthesis of polyelectrolyte-coated porphyrin nanospheres to reduce the toxicity of the surfactant as well as improve the biocompatibility of the nanospheres. The newly fabricated porphyrin nanospheres were characterized by TEM techniques, the electronic absorption spectra, photoluminescence emission spectra, dynamic light scattering, and cytotoxicity examination. The resulting nanospheres demonstrated good biocompatibility, excellent water dispersibility and low toxicity. In order to show their application in biophotonics, these porphyrin nanospheres were successfully applied in targeted living cancer cell imaging. The results showed an effective method had been explored to prepare water dispersible and highly stable porphyrin nanomaterial for biophotonics applications using hydrophobic porphyrin. The approach we reported shows obvious flexibility because the surfactants and polyelectrolytes can be optionally selected in accordance with the characteristics of the hydrophobic material. This strategy will expand the applications of hydrophobic porphyrins owning excellent properties in medicine and biology.

KEYWORDS: *hydrophobic porphyrin, polyelectrolyte, surfactant, layer-by-layer method, microemulsion method, biophotonics applications*
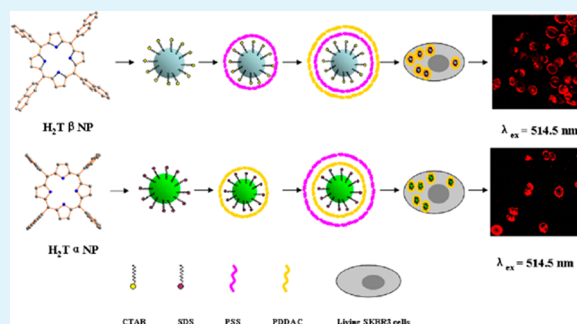
1. INTRODUCTION

Porphyrins and porphyrin derivatives are intensively investigated molecules owing to their remarkable photophysical, photochemical, electrochemical, and biochemical properties.[1−3] In recent years, porphyrin and porphyrin derivatives have attracted considerable research interests because of their promising application in biophotonics such as biological imaging and two-photon photodynamic therapy.[4−8] However, many porphyrins and porphyrin derivates are insoluble in water, which limits their application in medicine and biology. Therefore, it is important to explore suitable strategies to transform directly the hydrophobic porphyrins owning excellent properties into probes with excellent water dispersibility, good biocompatibility and bioenvironmental stability.

Chemical modification of porphyrins by attaching hydrophilic groups such as amine, carboxylic acid group, sulfonic acid group and glycosyl groups to the periphery positions of porphyrin is a commonly used approach to solve this problem.[9−11]

Recently, self-assembling of functional organic molecules into nanostructures has been explored widely in the field of material science and technology.[12−16] A variety of porphyrin-involved nanostructures, such as nanospheres, nanotubes, nanowires, nanowheels, nanorods, etc.[17−29] have been fabricated by various methods, including the sonication method, ionic self-assembly,

Scheme 1. Schematic Illustrations of Preparation of Porphyrin Nanospheres Using Hydrophobic Porphyrins
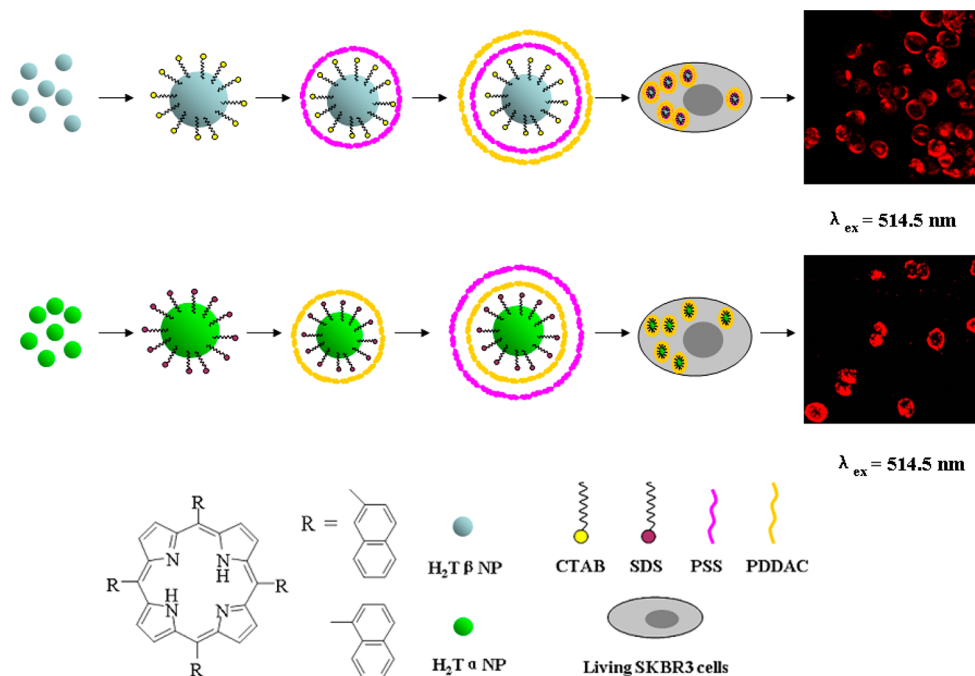
repreciptation, evaporation, surfactant-assisted self-assembly (SAS), etc.[30−35] These porphyrin-based nanostructures have gotten much more attention due to their potential applications in catalysis, optical device, storage, photovoltaics, field-effect transistor, and sensing.[36−43] However, most of the porphyrin-based nanostructures are not suitable for application in biology not only because many porphyrin-based nanostructures tend to aggregate in aqueous solutions but also because the size of the porphyrin-based nanostructures is difficult to control. In order to solve these problems, several porphyrin-based nanomaterials with good water dispersibility and bioenvironmental stability have been fabricated using different strategies. The Gong group developed a general method for preparation of porphyrin nanoparticles which is stable in water from porphyrins and (polyetheylene)glycol (PEG) derivatives.[44] Besides, porphyrin-doped conjugated polymer nanoparticles were prepared using a repreciptation method by Xu and co-workers.[45,46] However, all those structures have very limited dye-loading content and thus limited the brightness and singlet-oxygen production efficiency as photosensitizes. In addition, silica nanoparticles[47−49] loaded with organic molecules have been prepared to improve the hydrophilicity of organic molecules. However, due to the hydrophobic nature of organic molecules compared to the hydrophilic surface of silica, it seems difficult to fabricate silica nanoparticles loaded with organic molecules. Rossi prepared protoporphyrin IX nanoparticle carriers using a methodology that permits the photosensitizer to be firmly attached to the silica matrix through previous silyl modification of the porphyrin molecules.[50] Unfortunately, this method showed limitations because there must be a specific group on porphyrin which can be reacted with silane. Therefore, exploring alternative strategies for the design of porphyrins with good biocompatibility and excellent water dispersibility is highly desirable.

Herein we reported a novel and general method to prepare porphyrin nanospheres for biological applications using hydrophobic porphyrins. In order to display the generality of our method, we synthesized two hydrophobic porphyrin isomers, namely, meso-tetrakis(β-naphthyl)porphyrin (H$_2$TβNP) and meso-tetrakis(α-naphthyl)porphyrin (H$_2$TαNP) as starting material. The porphyrin isomers have been characterized by a series of spectroscopic methods. The structure of both porphyrin isomers showed completely different structures due to the different positions of the substitutes on the porphyrin ring which have been confirmed by X-ray diffraction analysis. The overall procedures for the fabrication of the porphyrin nanospheres are shown in Scheme 1. Briefly, the chloroform solution of the porphyrin together with appropriate aqueous solution of surfactant such as sodium dodecyl sulfate (SDS) and cetyltrimethylammonium bromide (CTAB) were mixed though sonication, then the chloroform was evaporated from the surfactant-stabilized oil-in-water microemulsion in which porphyrin molecules were well dispersed inside microemulsion droplets. Subsequently, the surfactant-stabilized nanospheres were coated with polyelectrolytes including poly(sodium-4-styrenesulfonate) (PSS) and poly(diallyldimethylammonium chloride) (PDDAC) through electrostatic interaction by layer-by-layer (LbL) method in order to reduce the toxicity of the surfactant as well as improve biocompatibility of the nanospheres. The newly fabricated porphyrin nanospheres were characterized by transmission electron microscope (TEM) techniques, the electronic absorption spectra, photoluminescence emission spectra, dynamic light scattering (DLS), and cytotoxicity examination. The resulting nanospheres demonstrated good biocompatibility, water dispersibility and low toxicity. In order to show their application in biophotonics, these porphyrin nanospheres were successfully applied in targeted living cancer cell imaging. Thus, it is expected that the method we reported will expand the applications of hydrophobic porphyrins owning excellent properties in biology and medicine.
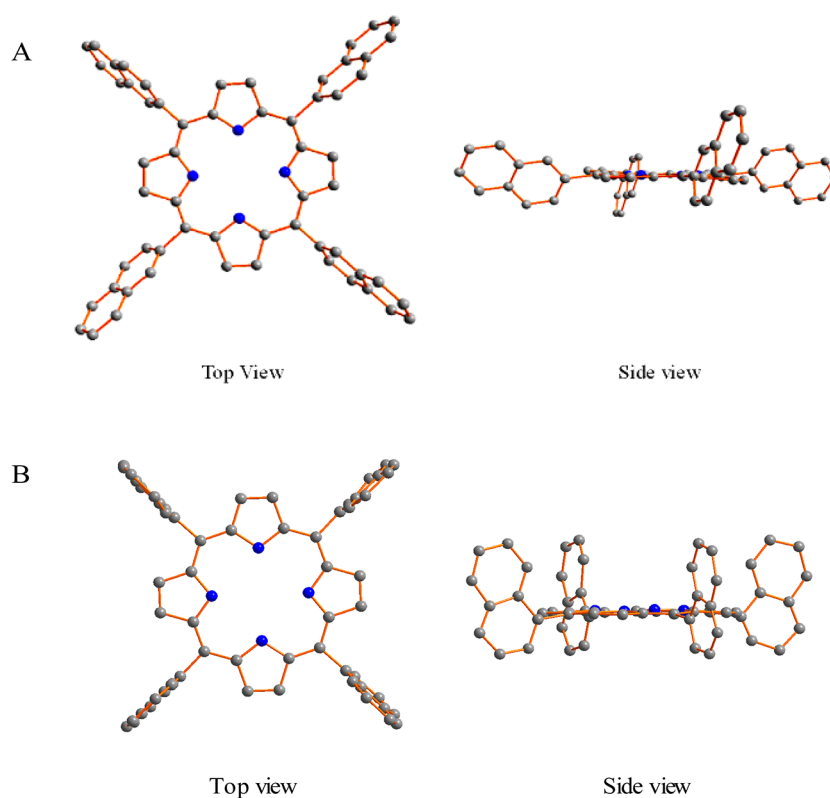
Figure 1. Molecular structures of H$_2$TβNP (A) and H$_2$TαNP (B) in top view and side view (C gray, N blue). Hydrogen atoms are omitted for clarity.

2. EXPERIMENTAL SECTION

2.1. Materials. 1-Naphthaldehyde, 2-naphthaldehyde, and pyrrole were purchased from J&K Scientific. Poly(sodium-4-styrenesulfonate) (PSS MW 70000), poly(diallyldimethylammonium chloride) (PDDAC MW 15000), sodium dodecyl sulfate (SDS), cetyltrimethylammonium bromide (CTAB) were purchased from Alfa Aesar. Sodium chloride (NaCl) was purchased from Guangdong Xilong Chemical Co., Ltd. Phosphate buffered saline (PBS, pH 7.4) was purchased from Beijing Biosynthesis Biotechnology Co., Ltd. Column chromatography was carried out on silica gel (Merck, Kieselgel 60, 70−230 mesh) with the indicated eluents. All other reagents and solvents were used as received. Deionized water (Millipore Milli-Q grade) with a resistivity of 18.2 MΩ/cm was used in all the experiments.

2.2. Characterization. Electronic absorption spectra were recorded with a Shimadzu UV-3600 spectrophotometer. Fluorescence experiments were performed with a RF-5301 PC spectrofluorophotometer. MALDI-TOF mass spectra were recorded on a Bruker Biflex III ultrahigh resolution mass spectrometer with α-cyano-4-hydroxycinnamic acid as the matrix. ^{1}H NMR spectra were recorded on a Bruker DPX 300 spectrometer (300 MHz) in CDCl$_3$, spectra were referenced internally by using the residual solvent resonance (δ = 7.26 for CDCl$_3$) relative to SiMe$_4$. Elemental analyses for C, H and N were performed with a Vario EL III elemental analyzer. Crystal data were collected on an Oxford Diffraction Gemini E diffractometer with Cu K$_\alpha$ radiation (λ = 1.5418 Å) at 150 K. TEM images were taken with a JEM-2100 electron microscope. Fluorescence imaging of cells was carried out using confocal microscopy (FV 1000, Olympus) under 514.5 nm laser excitation, and emission was collected in the range of 600−700 nm. Laser power was 2.3 mW at the sample position.

2.3. X-ray Diffraction Analysis. Crystal data of H$_2$TβNP and H$_2$TαNP were collected on an Oxford Diffraction Gemini E diffractometer with Cu Kα radiation (λ = 1.5418 Å) at 150 K. Final unit cell parameters were derived by global refinements of reflections obtained from integration of all the frame data. The collected frames were integrated by using the preliminary cell-orientation matrix.

CrysAlisPro Agilent Technologies software was used for collecting frames of data, indexing reflections, and determination of lattice constants; SHELXL was used for space group and structure determination, refinements, graphics, and structure reporting.[51] Anisotropic thermal parameters were used for the nonhydrogen atoms and isotropic parameters for the hydrogen atoms. CCDC 996151 for H$_2$TβNP and 1009202 for H$_2$TαNP, respectively, contain the supplementary crystallographic data for this paper and can be obtained free of charge from the Cambridge Crystallographic Data Centre via www.ccdc.cam.ac.uk/data_request/cif.

2.4. Intracellular Experiments. Human breast cancer cells (SKBR3) were purchased from China Type Culture Collection. SKBR3 cells were cultured at 37 °C in 5% CO$_2$ atmosphere. The culture media contain 10% fetal bovine serum (Gibco) and 1% penicillin-streptomycin (Nanjing KeyGen Biotech. Co., Ltd.). Cell viability was assessed with the 3-(4,5-dimethylthiazol-2-yl)-2,5-diphenyltetrazolium bromide (MTT, Sigma-Aldrich) assay. SKBR3 cells with a concentration of 10^4/mL were seeded into 96-well plates (100 μL/hole) and incubated for 24 h. Then, the porphyrin nanospheres or nanosphere-free controls were added, respectively, and incubated for 24 h. After that, 50 μL of four times diluted MTT solution was added into each well. After that the plate was further incubated for 4 h. After discarding the supernatant media, 150 μL of DMSO was added to each well. Finally, when the purple formazan crystals were dissolved by DMSO, the absorbance at 490 nm was recorded with a microplate reader (Bio-Rad 680). Cells incubated with pure culture media were used as the control.

2.5. Synthesis of H$_2$TβNP and H$_2$TαNP. The porphyrin isomers including H$_2$TβNP and H$_2$TαNP were prepared according to the modified published literature procedures.[52,53] Briefly, a mixture of freshly distilled β-naphthaldehyde (7.8 g, 0.05 mol) or α-naphthaldehyde (7.8 g, 0.05 mol) and pyrrole (3.35 g, 0.05 mol) in propyl acid (150 mL) was refluxed for 2 h, and after the solutions were cooled to room temperature, 400 mL of CH$_3$OH was added into the reaction mixture. The precipitate was filtered and washed with CH$_3$OH, then subjected to chromatography on a silica gel column

with $CHCl_3$ and petroleum ether (6:4) as eluent. After removing solvent in vacuo, the residue was rechromatographed under similar conditions followed by recrystallization from $CHCl_3/CH_3OH$ to give the target compounds (yield for $H_2T\beta NP$, 2.81g, 28%; $H_2T\alpha NP$, 2.1 g, 21%).

2.6. Preparation of $H_2T\beta NP/CTAB/PSS/PDDAC$ Nanospheres and $H_2T\alpha NP/SDS/PDDAC/PSS$ Nanospheres. The surfactant-stabilized nanospheres were prepared according to the modified published literature procedures.[54] In a 10 mL glass bottle, the mixture of 0.6 mL of $H_2T\beta NP$ (10^{-3} M in chloroform), and 5 mL of aqueous solution of CTAB (5×10^{-3} M) was emulsified by ultrasonic treatment for 3 min. The emulsion was subsequently heated at 60 °C for about 30 min to evaporate $CHCl_3$, and then the resulting transparent colloidal brown solution was obtained. The preparation of $H_2T\alpha NP/SDS$ nanospheres is similar to that of $H_2T\beta NP/CTAB$ nanospheres; the concentration of SDS is 3×10^{-3} M.

In order to reduce the cytotoxicity of CTAB and SDS effectively, two layers of polyelectrolytes were coated on the $H_2T\beta NP/CTAB$ nanospheres and $H_2T\alpha NP/SDS$ nanospheres.[55] $H_2T\beta NP/CTAB/PSS/PDDAC$ nanospheres and $H_2T\alpha NP/SDS/PDDAC/PSS$ nanospheres were prepared by the LbL approach.[55,56] A volume of 2 mL of $H_2T\beta NP/CTAB$ nanospheres containing excess CTAB was centrifuged once at 7000 rpm, after removing the upper layer solution, the nanospheres were dispersed in a solution containing 0.5 mL of PSS (10 mg/mL) and 5 mL of NaCl solution (1 mM), and then kept the solution standing for 1 h. The $H_2T\beta NP/CTAB/PSS$ were obtained after the excess polymer was removed by centrifugation. Subsequently, using the same strategy, the negative charged surface of $H_2T\beta NP/CTAB/PSS$ was further coated with a layer of positive PDDAC through electrostatic interaction. The preparation of $H_2T\alpha NP/SDS/PDDAC/PSS$ nanospheres is similar to that of $H_2T\beta NP/CTAB/PSS/PDDAC$ nanospheres.

3. RESULTS AND DISCUSSION

The porphyrin isomers meso-tetrakis(β-naphthyl)porphyrin ($H_2T\beta NP$) and meso-tetrakis(α-naphthyl)porphyrin ($H_2T\alpha NP$) were prepared in good yield according to the modified Adler−Longo method.[52,53] The yield of them is 28% for $H_2T\beta NP$ and 21% for $H_2T\alpha NP$, respectively. As mentioned in Table S2, the satisfactory elemental analysis results were obtained for these two prepared compounds. The MALDI-TOF mass spectra of them showed intense signal corresponding to the molecular ion M^+ (Figures S1 and S2). The ^1H NMR spectra of them recorded in $CDCl_3$ are shown in Figures S3 and S4.

In order to confirm the structures of the porphyrin isomers, the single crystals of them were obtained by slow diffusion of MeOH into the $CHCl_3$ solution. The porphyrin isomers showed different structures due to the different position of the naphthyl substitutes on the porphyrin ring. The porphyrin $H_2T\beta NP$ crystallizes in the monoclinic system with a $P121/n$ space group; in contrast, the porphyrin $H_2T\alpha NP$ crystallizes in the tetragonal system with a $I4/m$ space group. Crystallographic data and other pertinent information for them are summarized in Table S1. The molecular structures of them in two different perspective views are shown in Figure 1, from which their tetrapyrrole nature and in particular the positions of the substituent are clearly revealed. It can be seen that for $H_2T\beta NP$, the average dihedral angle of the tetrapyrrole ring and the naphthalene ring is about 63.6°, showing that the porphyrin is almost a rhombus on the top view; however, for porphyrin $H_2T\alpha NP$, the average dihedral angle of the tetrapyrrole ring with the naphthalene ring is about 90°, showing that the porphyrin is almost a perfect square on the top view.

Owing to the difference of molecular structure, we fabricated porphyrin nanospheres by the microemulsion method under different experimental conditions. The cation surfactant CTAB is used to prepare $H_2T\beta NP$ nanospheres; in contrast, the anionic surfactant SDS is used to prepare $H_2T\alpha NP$ nanospheres. Subsequently, in order to reduce the toxicity of the surfactant as well as improve the biocompatibility, the LbL method was used to coat the surfactant-stabilized nanospheres with the polyelectrolytes including PSS and PDDAC through electrostatic interaction. Although the LbL method has been used widely to modify the surface of Au, Ag, and other inorganic nanomaterial, this method has never been employed to modify the surface of porphyrin-based nanostructures. Figure 2 shows the TEM images of $H_2T\beta NP/CTAB/PSS/PDDAC$
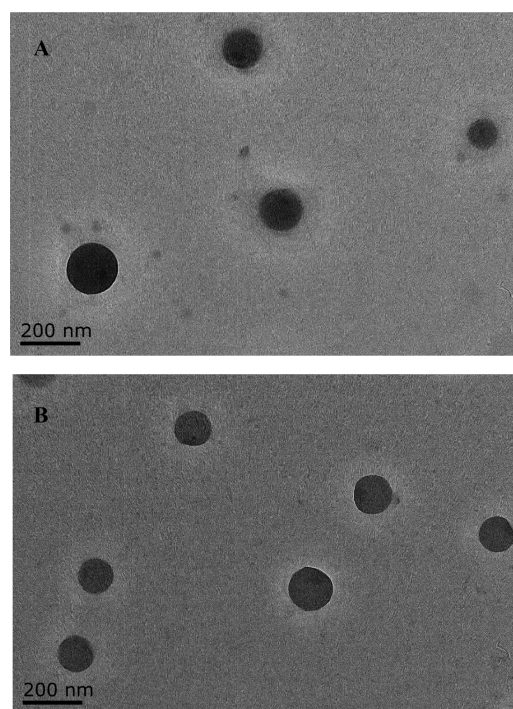
Figure 2. TEM images of (A) $H_2T\beta NP/CTAB/PSS/PDDAC$ nanospheres and (B) $H_2T\alpha NP/SDS/PDDAC/PSS$ nanospheres.

nanospheres and $H_2T\alpha NP/SDS/PDDAC/PSS$ nanospheres, and it can be seen that both of them are coated with polyelectrolyte and have uniform shape. As expected, when the excess surfactants were washed by water, nanospheres became agglomerated as shown in Figure S5. The average diameter is about 165 nm for $H_2T\beta NP/CTAB/PSS/PDDAC$ and 140 nm for $H_2T\alpha NP/SDS/PDDAC/PSS$ which are consistent with DLS analysis results (Figure S6). In order to further prove that the nanospheres are wrapped by polyelectrolyte, we examined the surface charge of the nanospheres before and after modification of polyelectrolyte by measuring the zeta-potentials. As shown in Figure 3, the z-potentials were 36 mV, −57.8 mV, 48.5 mV for the $H_2T\beta NP/CTAB$, $H_2T\beta NP/CTAB/PSS$, and $H_2T\beta NP/CTAB/PSS/PDDAC$ nanospheres, respectively; similarly, the zeta-potentials of $H_2T\alpha NP/SDS$, $H_2T\alpha NP/SDS/PDDAC$, and $H_2T\alpha NP/SDS/PDDAC/PSS$ nanospheres were −35.1 mV, 55.5 mV, and −36.4 mV, respectively. These results indicated that the polyelectrolyte was successfully modified onto the surfaces of the nanospheres. Because water dispersibility of porphyrin nanospheres is
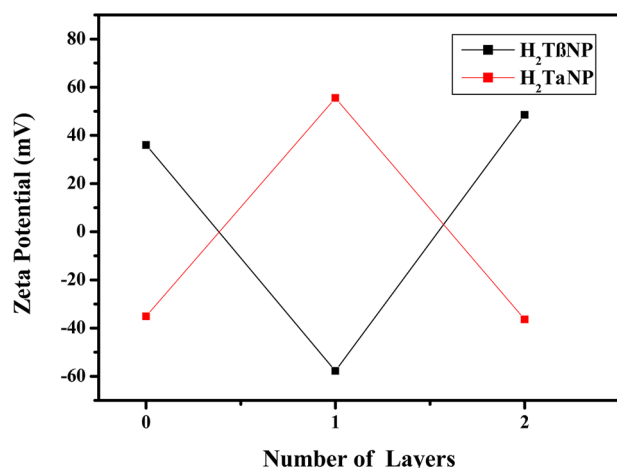
Figure 3. Z-potential data for porphyrin nanospheres at different stages of functionalization. 0 = CTAB or SDS; 1 = CTAB/PSS or SDS/PDDAC; 2 = CTAB/PSS/PDDAC or SDS/PDDAC/PSS.

important in biology application, the colloidal stability of $H_2T\beta NP$/CTAB/PSS/PDDAC nanospheres and $H_2T\alpha NP$/SDS/PDDAC/PSS nanospheres were evaluated using the DLS technique; compared with the fresh prepared nanospheres, the hydrodynamic diameters of $H_2T\beta NP$/CTAB/PSS/PDDAC nanospheres and $H_2T\alpha NP$/SDS/PDDAC/PSS nanospheres increased about 5% and 6%, respectively, after 4 days (Figure S7). The slight increase indicated that both of them showed good stability in deionized water. Surface charge repulsion between the polyelectrolyte coated nanospheres is an important factor to maintain them stable. Thus, it was demonstrated that surface modified by PSS and PDDAC can successfully achieve nanospheres with good stability and water dispersibility, which makes in vivo imaging possible.

The electronic absorption spectra of porphyrins in CHCl$_3$, surfactant-stabilized porphyrin nanospheres, and surfactant/polyelectrolyte modified porphyrin nanospheres are shown in Figure 4. Both porphyrins in CHCl$_3$ show typical bands of metal-free porphyrin compounds, and the absorption around 425 nm for $H_2T\beta NP$ and 424 nm for $H_2T\alpha NP$ can be attributed to the porphyrin Soret band, while the typical weak absorptions between 520 and 650 nm can be assigned to be the Q bands, respectively. As expected, the electronic absorption

spectra of porphyrin nanospheres are significantly different compared to the spectra of the corresponding porphyrin solutions. In comparison with the spectra of porphyrins in CHCl$_3$, the Soret bands are found to be broadened and split and both the Soret and Q bands of the nanostructures show significant red-shift, suggesting the formation of J-aggregates in these nanostructures according to the exciton theory.[57] It is worth noting that the packing mode of these reported nanospheres only exhibit J type aggregation, which can effectively reduce the fluorescence quenching.[57]

The photoluminescence (PL) emission spectra of porphyrins in CHCl$_3$ together with surfactant-stabilized porphyrin nanospheres and surfactant/polyelectrolyte modified porphyrin nanospheres are shown in Figure 5. As can be seen, upon excitation at 410 nm, the CHCl$_3$ solution of porphyrin show characteristic emission band with maxima at 656 nm for $H_2T\beta NP$ and 652 nm for $H_2T\alpha NP$, respectively. It is obvious that both of the emission bands of surfactant-stabilized porphyrin nanospheres and surfactant/polyelectrolyte modified porphyrin nanospheres are red-shifted as shown in Figure 5A,B, which corresponds to J-type aggregates and is in good agreement with the UV−vis spectra.[58] Compared with the absorption and photoluminescence spectra of surfactant-stabilized porphyrin nanospheres, the spectra of surfactant/polyelectrolyte modified porphyrin nanospheres show similar features, which indicate that the polyelectrolyte only increase the biocompatibility and reduced the toxicity of the nanospheres, whereas they do not affect the optical properties of porphyrin nanospheres.

The cytotoxicity of materials is crucial for their biological applications. In our experiments, PSS and PDDAC were modified onto the surface of the surfactant-stabilized porphyrin nanospheres by electrostatic interaction to reduce the cytotoxicity of SDS and CTAB.[59,60] To better investigate the influence of the outer PSS and PDDAC on cellular toxicity, the cytotoxicity of the $H_2T\beta NP$/CTAB nanospheres, $H_2T\beta NP$/CTAB/PSS/PDDAC nanospheres, $H_2T\alpha NP$/SDS nanospheres, and $H_2T\alpha NP$/SDS/PDDAC/PSS nanospheres were evaluated using an MTT viability assay. As shown in Figure 6, both surfactant-stabilized porphyrin nanospheres showed obvious cytotoxicity even at low concentration (2.5 μM), in contrast, for the cells treated with $H_2T\beta NP$/CTAB/PSS/PDDAC nanospheres and $H_2T\alpha NP$/SDS/PDDAC/PSS nanospheres, the relative viability was always high. Both $H_2T\beta NP$/
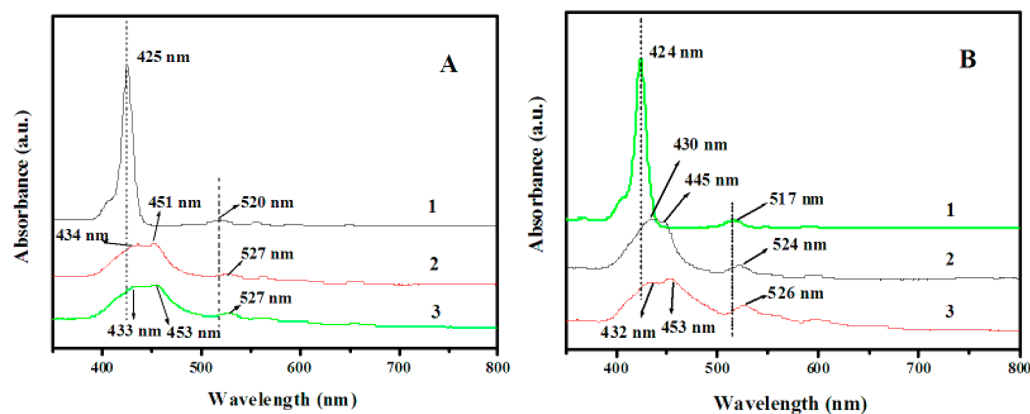

Figure 4. UV−vis absorption spectra of (A1) $H_2T\beta NP$ in CHCl$_3$, (A2) $H_2T\beta NP$/CTAB nanospheres, (A3) $H_2T\beta NP$/CTAB/PSS/PDDAC nanospheres; and (B1) $H_2T\alpha NP$ in CHCl$_3$, (B2) $H_2T\alpha NP$/SDS nanospheres, (B3) $H_2T\alpha NP$/SDS/PDDAC/PSS nanospheres. The concentrations were held at 10^{-6} mol/L.
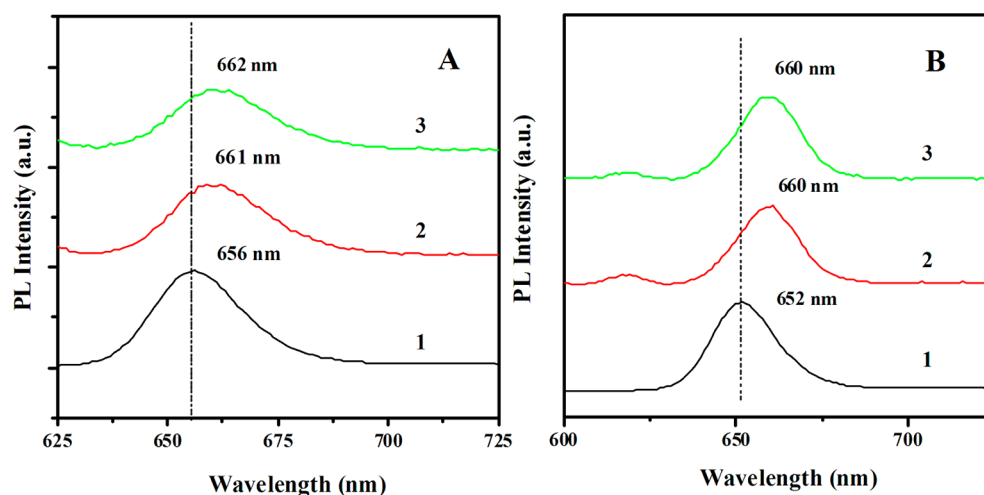
Figure 5. Photoluminescence (PL) spectra of (A1) H$_2$TβNP in CHCl$_3$, (A2) H$_2$TβNP/CTAB nanospheres, (A3) H$_2$TβNP/CTAB/PSS/PDDAC nanospheres; (B1) H$_2$TαNP in CHCl$_3$, (B2) H$_2$TαNP/SDS nanospheres, (B3) H$_2$TαNP/SDS/PDDAC/PSS nanospheres.
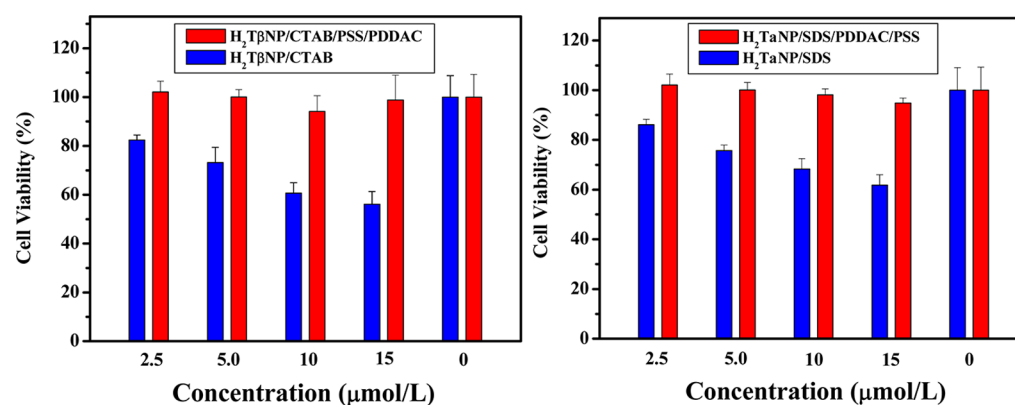

Figure 6. Viability of SKBR3 cells exposed to H$_2$TβNP/CTAB nanospheres, H$_2$TβNP/CTAB/PSS/PDDAC nanospheres (left) and H$_2$TαNP/SDS nanospheres, H$_2$TαNP/SDS/PDDAC/PSS nanospheres (right) for 24 h.

CTAB/PSS/PDDAC nanospheres and H$_2$TαNP/SDS/PDDAC/PSS nanospheres displayed good cytocompatibility as expected. When the concentration of the nanocomposites increased up to 15 μM, the cell viability was still more than 87%. These results demonstrated the cytocompatibility of these polyelectrolyte coated nanospheres, highlighting their potential for cellular imaging.

The newly fabricated porphyrin nanospheres with good water dispersibility and bioenvironmental stability are expected to be used in biophotonics; therefore, the living cancer cell imaging experiments were conducted to demonstrate their application in biophotonics. Figure 7 shows the fluorescent microscopic images of live SKBR3 cells incubated with H$_2$TβNP/CTAB/PSS/PDDAC or H$_2$TαNP/SDS/PDDAC/PSS nanospheres for 12 h, and an excitation wavelength of 514.5 nm was used. It can be seen that the luminescence from these porphyrin nanospheres was stable and bright, leading to high-contrast cellular imaging. The morphology of the live SKBR3 cells can be observed clearly, which indicates that these porphyrin nanospheres are favorable for biophotonic applications.

4. CONCLUSIONS

In summary, we reported a novel and general strategy to fabricate water dispersible and stable porphyrin nanospheres for
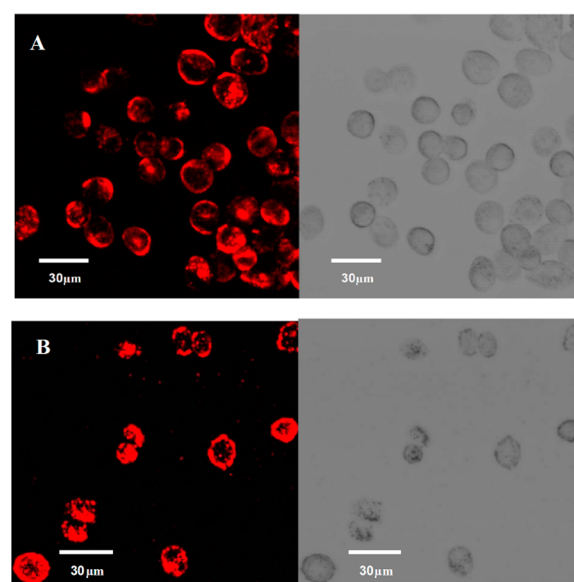

Figure 7. Confocal images of SKBR3 cells incubated with the H$_2$TβNP/CTAB/PSS/PDDAC nanospheres (A) and H$_2$TαNP/SDS/PDDAC/PSS nanospheres (B). (Left, fluorescence images; right, bright field images).

bioapplications using hydrophobic porphyrin. The hydrophobic porphyrins with different molecular structures were fabricated into surfactant stabilized nanospheres, and then they were surface modified with polyelectrolyte through electrostatic interaction to achieve good water dispersibility and bioenvironmental stability. These nanospheres were successfully applied in biophotonics such as targeted cell imaging. The approach we reported shows obvious flexibility because the surfactants and polyelectrolyte can be optionally selected in accordance with the characteristics of the hydrophobic material. This strategy will expand the applications of hydrophobic porphyrins owning excellent properties in medicine and biology. Future work in our group will include fabricating porphyrin nanomaterials owning a high two-photon absorption (2PA) cross section by our strategy and testing these nanomaterials for 2PA PDT.

■ ASSOCIATED CONTENT

Ⓢ Supporting Information

The Supporting Information is available free of charge on the ACS Publications website at DOI: 10.1021/acsami.5b05256.

> MALDI-TOF mass spectra, ^{1}H NMR spectra, crystallographic data, TEM images, and hydrodynamic diameters (PDF)
> Crystallographic data for H$_2$TβNP (CIF)
> Crystallographic data for H$_2$TαNP (CIF)

■ AUTHOR INFORMATION

Corresponding Author
*Phone: +86 25 83792470. Fax: +86 025 83790201. E-mail: cyp@seu.edu.cn.

Notes
The authors declare no competing financial interest.

■ ACKNOWLEDGMENTS

■ REFERENCES

(1) Kadish, K. M., Smith, K. M., Guilard, R., Eds. *The Porphyrin Handbook*; Academic Press: San Diego, CA, 2000; Vol. 6, p 346.

(2) Makiura, R.; Motoyama, S.; Umemura, Y.; Yamanaka, H.; Sakata, O.; Kitagawa, H. Surface Nano-Architecture of a Metal-Organic Framework. *Nat. Mater.* 2010, 9, 565−571.

(3) Lovell, J. F.; Jin, C. S.; Huynh, E.; Jin, H.; Kim, C.; Rubinstein, J. L.; Chan, W. C.W.; Cao, W.; Wang, L. V.; Zheng, G. Porphysome Nanovesicles Generated by Porphyrin Bilayers for Use as Multimodal Biophotonic Contrast Agents. *Nat. Mater.* 2011, 10, 324−332.

(4) Kim, K. S.; Lim, J. M.; Osuka, A.; Kim, D. Various Strategies for Highly-Efficient Two-Photon Absorption in Porphyrin Arrays. *J. Photochem. Photobiol., C* 2008, 9, 13−28.

(5) Starkey, J. R.; Rebane, A. K.; Drobizhev, M. A.; Meng, F.; Gong, A.; Elliott, A.; McInnerney, K.; Spangler, C. W. New Two-Photon Photodynamic Therapy Sensitizers Induce Xenograft Tumor Regressions After NIR Laser Treatment Through the Body of the Host Mouse. *Clin. Cancer Res.* 2008, 14, 6564−6573.

(6) Collins, H. A.; Khurana, M.; Moriyama, E. H.; Mariampillai, A.; Dahlstedt, E.; Balaz, M.; Kuimova, M. K.; Drobizhev, M.; Yang, X. D.; Phillips, D.; Rebane, A.; Wilson, B. C.; Anderson, H. L. Blood-Vessel Closure Using Photosensitizers Engineered for Two-Photon Excitation. *Nat. Photonics* 2008, 2, 420−424.

(7) Dahlstedt, E.; Collins, H. A.; Balaz, M.; Kuimova, M. K.; Khurana, M.; Wilson, B. C.; Phillips, D.; Anderson, H. L. One- and Two-Photon Activated Phototoxicity of Conjugated Porphyrin Dimers with High Two-Photon Absorption Cross Sections. *Org. Biomol. Chem.* 2009, 7, 897−904.

(8) Dy, J. T.; Ogawa, K.; Satake, A.; Ishizumi, A.; Kobuke, Y. Water-Soluble Self-Assembled Butadiyne-Bridged Bisporphyrin: A Potential Two-Photon-Absorbing Photosensitizer for Photodynamic Therapy. *Chem. - Eur. J.* 2007, 13, 3491−3500.

(9) Kuimova, M. K.; Collins, H. A.; Balaz, M.; Dahlstedt, E.; Levitt, J. A.; Sergent, N.; Suhling, K.; Drobizhev, M.; Makarov, N. S.; Rebane, A.; Anderson, H. L.; Phillips, D. Photophysical Properties and Intracellular Imaging of Water-Soluble Porphyrin Dimers for Two-photon Excited Photodynamic Therapy. *Org. Biomol. Chem.* 2009, 7, 889−896.

(10) Ogawa, K.; Kobuke, Y. Design of Two-Photon Absorbing Materials for Molecular Optical Memory and Photodynamic Therapy. *Org. Biomol. Chem.* 2009, 7, 2241−2246.

(11) Balaz, M.; Collins, H. A.; Dahlstedt, E.; Anderson, H. L. Synthesis of Hydrophilic Conjugated Porphyrin Dimers for One-Photon and Two-Photon Photodynamic Therapy at NIR wavelengths. *Org. Biomol. Chem.* 2009, 7, 874−888.

(12) Cui, Q. L.; He, F.; Wang, X. Y.; Xia, B. H.; Li, L. D. Gold Nanoflower@Gelatin Core−Shell Nanoparticles Loaded with Conjugated Polymer Applied for Cellular Imaging. *ACS Appl. Mater. Interfaces* 2013, 5, 213−219.

(13) Chan, W. C. W.; Nie, S. Quantum Dot Bioconjugates for Ultrasensitive Nonisotopic Detection. *Science* 1998, 281, 2016−2018.

(14) Pansare, V. J.; Hejazi, S.; Faenza, W. J.; Prud'homme, R. K. Review of Long-Wavelength Optical and NIR Imaging Materials: Contrast Agents, Fluorophores, and Multifunctional Nano Carriers. *Chem. Mater.* 2012, 24, 812−827.

(15) Tsay, J. M.; Trzoss, M.; Shi, L. X.; Kong, X. X.; Selke, M.; Jung, M. E.; Weiss, S. Singlet Oxygen Production by Peptide-Coated Quantum Dot-Photosensitizer Conjugates. *J. Am. Chem. Soc.* 2007, 129, 6865−6871.

(16) Zenkevich, E. I.; Sagun, E. I.; Knyukshto, V. N.; Stasheuski, A. S.; Galievsky, V. A.; Stupak, A. P.; Blaudeck, T.; von Borczyskowski, C. Quantitative Analysis of Singlet Oxygen (^{1}O$_2$) Generation via Energy Transfer in Nanocomposites Based on Semiconductor Quantum Dots and Porphyrin Ligands. *J. Phys. Chem. C* 2011, 115, 21535−21545.

(17) Hu, J. S.; Guo, Y. G.; Liang, H. P.; Wan, L. J.; Jiang, L. Three-Dimensional Self-Organization of Supramolecular Self-Assembled Porphyrin Hollow Hexagonal Nanoprisms. *J. Am. Chem. Soc.* 2005, 127, 17090−17095.

(18) Lee, S. J.; Hupp, J. T.; Nguyen, S. T. Growth of Narrowly Dispersed Porphyrin Nanowires and Their Hierarchical Assembly into Macroscopic Columns. *J. Am. Chem. Soc.* 2008, 130, 9632−9633.

(19) Hasobe, T.; Sandanayaka, A. S. D.; Wada, T.; Araki, Y. Fullerene-encapsulated Porphyrin Hexagonal Nanorods. An Anisotropic Donor−Acceptor Composite for Efficient Photoinduced Electron Transferand Light Energy Conversion. *Chem. Commun.* 2008, 3372−3374.

(20) Drain, C. M.; Varotto, A.; Radivojevic, I. Self-Organized Porphyrinic Materials. *Chem. Rev.* 2009, 109, 1630−1658.

(21) Balaban, T. S. Tailoring Porphyrins and Chlorins for Self-Assembly in Biomimetic Artificial Antenna Systems. *Acc. Chem. Res.* 2005, 38, 612−623.

(22) van Hameren, R.; Schön, P.; van Buul, A. M.; Hoogboom, J.; Lazarenko, S. V.; Gerritsen, J. W.; Engelkamp, H.; Christianen, P. C. M.; Heus, H. A.; Maan, J. C.; Rasing, T.; Speller, S.; Rowan, A. E.; Elemans, J. A. A. W.; Nolte, R. J. M. Macroscopic Hierarchical Surface Patterning of Porphyrin Trimers via Self-Assembly and Dewetting. *Science* 2006, 314, 1433−1436.

(23) Li, M.; den Boer, D.; Iavicoli, P.; Adisoejoso, J.; Uji-i, H.; Van der Auweraer, M.; Amabilino, D. B.; Elemans, J. A. A. W.; De Feyter, S.

Tip-Induced Chemical Manipulation of Metal Porphyrins at a Liquid/Solid Interface. *J. Am. Chem. Soc.* **2014**, *136*, 17418−17421.

(24) Bai, F.; Sun, Z.; Wu, H. M.; Haddad, R. E.; Coker, E. N.; Huang, J. Y.; Rodriguez, M. A.; Fan, H. Y. Porous One-Dimensional Nanostructures Through Confined Cooperative Self-Assembly. *Nano Lett.* **2011**, *11*, 5196−5200.

(25) Gao, Y.; Zhang, X.; Ma, C.; Li, X.; Jiang, J. Morphology-Controlled Self-Assembled Nanostructures of 5,15- Di[4-(5-acetylsulfanylpentyloxy)phenyl] porphyrin Derivatives. Effect of Metal-Ligand Coordination Bonding on Tuning the Intermolecular Interaction. *J. Am. Chem. Soc.* **2008**, *130*, 17044−17052.

(26) Doan, S. C.; Shanmugham, S.; Aston, D. E.; McHale, J. L. Counterion Dependent Dye Aggregates: Nanorods and Nanorings of Tetra(*p*-carboxyphenyl)porphyrin. *J. Am. Chem. Soc.* **2005**, *127*, 5885−5892.

(27) Shirakawa, M.; Fujita, N.; Shinkai, S. A Stable Single Piece of Unimolecularly π-Stacked Porphyrin Aggregate in a Thixotropic Low Molecular Weight Gel: A One-Dimensional Molecular Template for Polydiacetylene Wiring up to Several Tens of Micrometers in Length. *J. Am. Chem. Soc.* **2005**, *127*, 4164−4165.

(28) Lee, S. J.; Malliakas, C. D.; Kanatzidis, M. G.; Hupp, J. T.; Nguyen, S. T. Amphiphilic Porphyrin Nanocrystals: Morphology Tuning and Hierarchical Assembly. *Adv. Mater.* **2008**, *20*, 3543−3549.

(29) Jang, J. H.; Jeon, K.-S.; Oh, S.; Kim, H.-J.; Asahi, T.; Masuhara, H.; Yoon, M. Synthesis of Sn-Porphyrin-Intercalated Trititanate Nanofibers: Optoelectronic Properties and Photocatalytic Activities. *Chem. Mater.* **2007**, *19*, 1984−1991.

(30) Borras, A.; Aguirre, M.; Groening, O.; Lopez-Cartes, C.; Groening, P. Synthesis of Supported Single-Crystalline Organic Nanowires by Physical Vapor Deposition. *Chem. Mater.* **2008**, *20*, 7371−7373.

(31) Kishida, T.; Fujita, N.; Sada, K.; Shinkai, S. Sol−Gel Reaction of Porphyrin-Based Superstructures in the Organogel Phase: Creation of Mechanically Reinforced Porphyrin Hybrids. *J. Am. Chem. Soc.* **2005**, *127*, 7298−7299.

(32) Hasobe, T.; Oki, H.; Sandanayaka, A. S. D.; Murata, H. Sonication-Assisted Supramolecular Nanorods of *meso*-Diaryl-Substituted Porphyrins. *Chem. Commun.* **2008**, 724−726.

(33) Wang, Z.; Medforth, C. J.; Shelnutt, J. A. Porphyrin Nanotubes by Ionic Self-Assembly. *J. Am. Chem. Soc.* **2004**, *126*, 15954−15955.

(34) Wang, Z.; Li, Z.; Medforth, C. J.; Shelnutt, J. A. Self-Assembly and Self-Metallization of Porphyrin Nanosheets. *J. Am. Chem. Soc.* **2007**, *129*, 2440−2441.

(35) Yoon, S. M.; Hwang, I. C.; Kim, K. S.; Choi, H. C. Synthesis of Single-Crystal Tetra(4-pyridyl)porphyrin Rectangular Nanotubes in the Vapor Phase. *Angew. Chem., Int. Ed.* **2009**, *48*, 2506−2509.

(36) Schwab, A. D.; Smith, D. E.; Bond-Watts, B.; Johnston, D. E.; Hone, J.; Johnson, A. T.; de Paula, J. C.; Smith, W. F. Photoconductivity of Self-Assembled Porphyrin Nanorods. *Nano Lett.* **2004**, *4*, 1261−1265.

(37) Mandal, S.; Bhattacharyya, S.; Borovkov, V.; Patra, A. Porphyrin-Based Functional Nanoparticles: Conformational and Photophysical Properties of Bis-Porphyrin and Bis-Porphyrin Encapsulated Polymer Nanoparticles. *J. Phys. Chem. C* **2011**, *115*, 24029−24036.

(38) Mandal, S.; Bhattacharyya, S.; Borovkov, V.; Patra, A. Photophysical Properties, Self-Assembly Behavior, and Energy Transfer of Porphyrin-Based Functional Nanoparticles. *J. Phys. Chem. C* **2012**, *116*, 11401−11407.

(39) Arai, T.; Tanaka, M.; Kawakami, H. Porphyrin-Containing Electrospun Nanofibers: Positional Control of Porphyrin Molecules in Nanofibers and Their Catalytic Application. *ACS Appl. Mater. Interfaces* **2012**, *4*, 5453−5457.

(40) Huang, C.; Li, Y.; Song, Y.; Li, Y.; Liu, H.; Zhu, D. Ordered Nanosphere Alignment of Porphyrin for the Improvement of Nonlinear Optical Properties. *Adv. Mater.* **2010**, *22*, 3532−3536.

(41) Wang, L.; Chen, Y.; Jiang, J. Controlling the Growth of Porphyrin Based Nanostructures for Tuning Third-Order Optical Properties. *Nanoscale* **2014**, *6*, 1871−1878.

(42) Guo, P.; Zhao, G.; Chen, P.; Lei, B.; Jiang, L.; Zhang, H.; Hu, W.; Liu, M. Porphyrin Nanoassemblies via Surfactant-Assisted Assembly and Single Nanofiber Nanoelectronic Sensors for High-Performance H_2O_2 Vapor Sensing. *ACS Nano* **2014**, *8*, 3402−3411.

(43) Wang, Z.; Ho, K. J.; Medforth, C. J.; Shelnutt, J. A. Porphyrin Nanofiber Bundles from Phase-Transfer Ionic Self-Assembly and Their Photocatalytic Self-Metallization. *Adv. Mater.* **2006**, *18*, 2557−2560.

(44) Gong, X. C.; Milic, T.; Xu, C.; Batteas, J. D.; Drain, C. M. Preparation and Characterization of Porphyrin Nanoparticles. *J. Am. Chem. Soc.* **2002**, *124*, 14290−14291.

(45) Shen, X.; He, F.; Wu, L. H.; Xu, G. Q.; Yao, S. Q.; Xu, Q. H. Enhanced Two-Photon Singlet Oxygen Generation by Photosensitizer-Doped Conjugated Polymer Nanoparticles. *Langmuir* **2011**, *27*, 1739−1744.

(46) Wu, C.; Xu, Q. H. Enhanced One- and Two-Photon Excitation Emission of a Porphyrin Photosensitizer by FRET from a Conjugated Polyelectrolyte. *Macromol. Rapid Commun.* **2009**, *30*, 504−508.

(47) He, X. X.; Wang, Y. S.; Wang, K. M.; Chen, M.; Chen, S. Y. Fluorescence Resonance Energy Transfer Mediated Large Stokes Shifting Near-Infrared Fluorescent Silica Nanoparticles for in Vivo Small-Animal Imaging. *Anal. Chem.* **2012**, *84*, 9056−9064.

(48) Wu, X.; Chang, S.; Sun, X. R.; Guo, Z. Q.; Li, Y. S.; Tang, J. B.; Shen, Y. Q.; Shi, J. L.; Tian, H.; Zhu, W. H. Constructing NIR Silica−Cyanine Hybrid Nanocomposite for Bioimaging *in vivo*: a Breakthrough in Photo-Stability and Bright Fluorescence with Large Stokes Shift. *Chem. Sci.* **2013**, *4*, 1221−1228.

(49) Gorelikov, I.; Matsuura, N. Single-Step Coating of Mesoporous Silica on Cetyltrimethyl Ammonium Bromide-Capped Nanoparticles. *Nano Lett.* **2008**, *8*, 369−373.

(50) Rossi, L. M.; Silva, P. R.; Vono, L. L.; Fernandes, A. U.; Tada, D. B.; Baptista, M. S. Protoporphyrin IX Nanoparticle Carrier: Preparation, Optical Properties, and Singlet Oxygen Generation. *Langmuir* **2008**, *24*, 12534−12538.

(51) Sheldrick, G. M. *SHELX-97*; Universität Göttingen: Göttingen, Germany, 1997.

(52) Adler, A. D.; Longo, F. R.; Finarelli, J. D.; Goldmacher, J.; Assour, J.; Korsakoff, L. A Simplified Synthesis for Meso-Tetraphenylporphine. *J. Org. Chem.* **1967**, *32*, 476−480.

(53) George, R. G.; Padmanabhan, M. Studies on Some New *meso*-Aryl Substituted Octabromo-Porphyrins and Their Zn(II) Derivatives. *Polyhedron* **2003**, *22*, 3145−3154.

(54) Zhong, Y.; Wang, Z. X.; Zhang, R. F.; Bai, F.; Wu, H. M.; Haddad, R.; Fan, H. Y. Interfacial Self-Assembly Driven Formation of Hierarchically Structured Nanocrystals with Photocatalytic Activity. *ACS Nano* **2014**, *8*, 827−833.

(55) Ding, H.; Yong, K. T.; Roy, I.; Pudavar, H. E.; Law, W. C.; Bergey, E. J.; Prasad, P. N. Gold Nanorods Coated with Multilayer Polyelectrolyte as Contrast Agents for Multimodal Imaging. *J. Phys. Chem. C* **2007**, *111*, 12552−12557.

(56) Gole, A.; Murphy, C. J. Polyelectrolyte-Coated Gold Nanorods: Synthesis, Characterization and Immobilization. *Chem. Mater.* **2005**, *17*, 1325−1330.

(57) Verma, S.; Ghosh, A.; Das, A.; Ghosh, H. N. Ultrafast Exciton Dynamics of J- and H-Aggregates of the Porphyrin-Catechol in Aqueous Solution. *J. Phys. Chem. B* **2010**, *114*, 8327−8334.

(58) Mandal, S.; Nayak, S. K.; Mallampalli, S.; Patra, A. Surfactant-Assisted Porphyrin Based Hierarchical Nano/Micro Assemblies and Their Efficient Photocatalytic Behavior. *ACS Appl. Mater. Interfaces* **2014**, *6*, 130−136.

(59) Wang, Z. Y.; Zong, S. F.; Yang, J.; Song, C. Y.; Li, J.; Cui, Y. P. One-step Functionalized Gold Nanorods as Intracellular Probe with Improved SERS Performance and Reduced Cytotoxicity. *Biosens. Bioelectron.* **2010**, *26*, 241−247.

(60) Connor, E. E.; Mwamuka, J.; Gole, A.; Murphy, C. J.; Wyatt, M. D. Gold Nanoparticles Are Taken Up by Human Cells but Do Not Cause Acute Cytotoxicity. *Small* **2005**, *1*, 325−327.